J Paleolimnol (2021) 65:255–269
https://doi.org/10.1007/s10933-020-00169-3

ORIGINAL PAPER

Impacts of Norse settlement on terrestrial and aquatic ecosystems in Southwest Iceland

Nora Richter · James M. Russell · Johanna Garfinkel · Yongsong Huang

Received: 28 January 2020 / Accepted: 7 December 2020 / Published online: 4 January 2021

Abstract Norse colonization of North Atlantic islands in the 1st millennium of the Common Era led to drastic prehistoric environmental changes in these previously "pristine" landscapes. In Iceland, Norse settlement is associated with a rapid decline in birch trees and heightened soil erosion, yet the timing of Norse exploration in the North Atlantic coincided with large climate changes that also influenced Icelandic environments. To date, there are few records that disentangle climatic and human impacts on terrestrial ecosystems, and there has been very little work on the impacts of Norse arrival on Iceland's aquatic ecosystems. Here we use a high-resolution lake-sediment record from Vestra Gíslholtsvatn (VGHV), southwest Iceland to investigate these processes during the last 2,000 years. Norse arrival (c. 870 CE) in Iceland is followed by a rapid increase in sedimentation rate and a transition in leaf wax *n*-alkanes indicating a decrease in trees and expansion of grasses. This transition coincides with limnological changes, including increased primary productivity (i.e. C_{17} *n*-alkane and biogenic opal fluxes) and shifts in the haptophyte algal community. Many of these changes are still apparent today. Comparisons with a new winter-spring alkenone temperature reconstruction from VGHV and marine sea surface temperature records show little to no correlation between terrestrial and aquatic ecological changes and climate at this time. Similarly, volcanic eruptions recorded in VGHV are not associated with any long-term environmental changes. Rather, the VGHV record suggests that human settlement had a lasting impact on the catchment area of VGHV and changes within the lake ecosystem.

Keywords Paleolimnology · Paleoecology · Alkenone · n-alkane · Common Era

Introduction

Norse colonization, or *landnám*, of North Atlantic lands occurred during a warmer, Medieval climate that allowed the Norse to reach and settle the Faroe Islands (between c. 800 and 850 CE), Iceland (c. 874 CE), and eventually Greenland (c. 985 CE) (Richards 2005). *Landnám* had major environmental consequences in Iceland and Greenland as the settlers imposed Norse agricultural practices on these new landscapes (Dugmore et al. 2005). Settlements in Iceland withstood variations in climate and other environmental changes,

N. Richter (✉) · J. M. Russell · J. Garfinkel · Y. Huang
Department of Earth, Environmental and Planetary Sciences, Brown University, Providence, RI 02912, USA
e-mail: nora_richter@alumni.brown.edu

N. Richter
The Josephine Bay Paul Center for Comparative Molecular Biology and Evolution, Marine Biological Laboratory, Woods Hole, MA 02543, USA

including volcanic eruptions and landscape degradation, whereas Greenlandic settlements were abandoned within a few centuries (Dugmore et al. 2005). Today, Iceland is still faced with environmental issues that were triggered by the Norse, but it is unclear how climate change and on-going human activities will continue to alter terrestrial and aquatic ecosystems. Thus, there is a need to understand the role of humans relative to past climate variability in shaping the modern-day landscape of Iceland.

Prior to human settlement, birch forests were dominant in the southern Icelandic lowlands, yet it is unclear how widespread or stable these forests were in the face of climate change before c. 870 CE (Ólafsdóttir et al. 2001; Dugmore et al. 2005; Streeter et al. 2015). Upon arrival in Iceland and Greenland, Norse settlers cut birch trees to clear space for agriculture and for use as building materials and fuel sources (Hallsdóttir 1987; Dugmore et al. 2005; Massa et al. 2012a). Persistent grazing by cattle and sheep prevented reforestation, and contributed to the expansion of grasses, sedges, and weeds that are still apparent in the present-day vegetation (Dugmore et al. 2005; Hallsdóttir and Caseldine 2005). Although there is evidence that soil erosion rates were already high prior to *landnám* (Geirsdóttir et al. 2009, 2013), breaks in vegetation and soil tilling for agriculture contributed to accelerated soil erosion in Iceland (Dugmore et al. 2009). However, other studies suggest that heightened soil erosion only became a problem during the Little Ice Age as the climate cooled (Geirsdóttir et al. 2009, 2013). These interpretations are complicated by not accounting for changes in sedimentation rates and the use of proxies that are subject to multiple environmental and climatic factors.

Numerous studies have focused on changes in the terrestrial landscape during *landnám*, yet the resulting human and climate impacts on lacustrine ecosystems are poorly understood despite being an important resource for the Icelandic community. For instance, in northern Iceland and in the Faroe Islands, primary productivity in lakes increased shortly after Norse settlement, potentially due to nutrient loading (Hannon et al. 2005; Lawson et al. 2007). However, proxies for primary productivity (e.g. biogenic silica), which are potentially sensitive to human-driven changes over the past millennia, are often interpreted as records of climate change (e.g. temperature) (Geirsdóttir et al. 2009, 2013; Blair et al. 2015).

In this study, we use a high-resolution lake sediment record with a well-constrained age model from southwest Iceland to assess the impacts of climate change relative to human disturbances on the terrestrial landscape and aquatic ecosystems over the last 2,000 years. Our paleoecological record from Vestra Gíslholtsvatn (VGHV) utilizes proxies that directly reflect the magnitude of vegetation changes, the onset of heightened soil erosion, and variability in primary productivity. In addition, we use an alkenone paleothermometer to develop a high-resolution temperature record from the same core that allows us to differentiate climate changes from human impacts on the environment.

Study site

VGHV is a small lake (1.57 km^2) in southwest Iceland (61 m a.s.l., 63°56′ N, 20°31′ W) that is situated near some of the initial Norse settlements (Fig. 1). The lake has no large inlets or outlets and sits on bedrock consisting of basalt (Hjartarson and Sæmundsson 2014; Blair et al. 2015). Pollen records from VGHV suggest that the landscape around the lake was dominated by birch trees prior to 874 $\pm$ 2 CE, whereas today the catchment is used for planting hayfields and sheep grazing (Hallsdóttir and Caseldine 2005; Blair et al. 2015). An 8.14-m-long lake sediment core was retrieved from VGHV in 2008 using a Bolivia piston coring system (Blair et al. 2015). Although the core consists of six 1.5-m sections, we only focus on the first two sections of the core in this study. The cores were previously analyzed and are currently archived at the National Lacustrine Core Facility (LacCore) at the University of Minnesota (Blair et al. 2015). In 2018, the first two sections of the core were sampled at 2-cm increments for lipid analysis.

Methods

Age model

The sediment cores from VGHV were previously dated using tephras (Fig. 2). The tephra layers in VGHV were previously geochemically analyzed using an Electron Microprobe Analyzer, and the resulting geochemical fingerprints were compared with well-

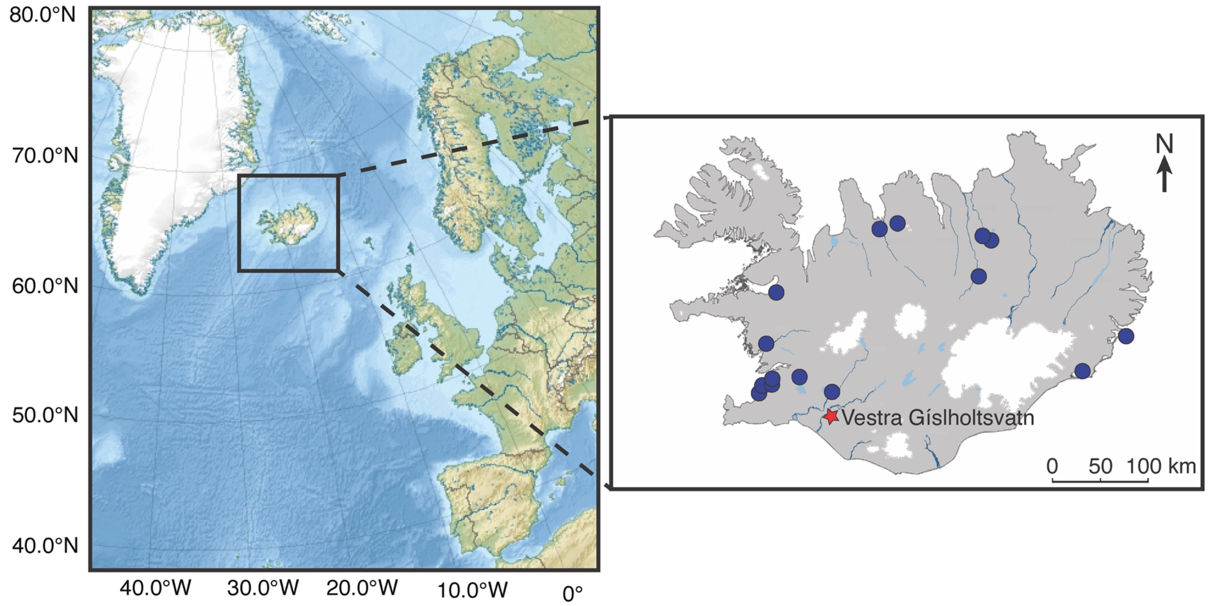

Fig. 1 Map of Iceland with the study site, Vestra Gíslholtsvatn (VGHV), indicated by a red star. The blue circles correspond to initial Norse settlements (Zori 2016). Raster data for the maps are from the National Land Survey of Iceland and Natural Earth. Maps were rendered in Matlab. (Color figure online)

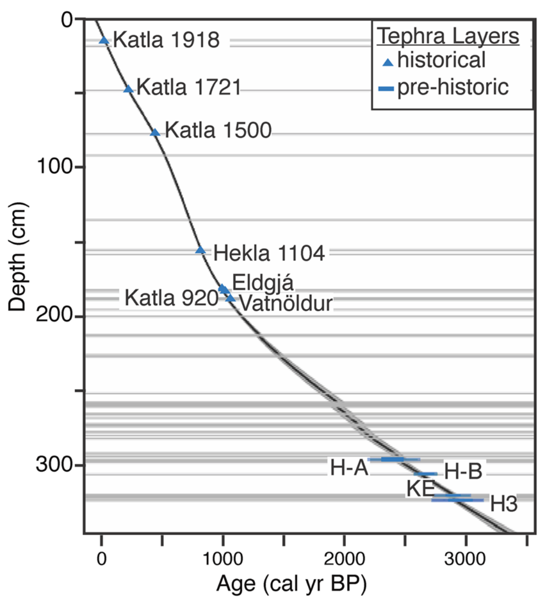

Fig. 2 VGHV age model with historic and pre-historic tephras. Tephra slumps that were removed from analysis are indicated by gray lines. (Color figure online)

constrained records of tephrostratigraphy from Iceland (Christensen 2013; Blair et al. 2015). Seven historically recorded tephras and four pre-historical tephras were identified during the last 3,000 years. The age model for this study was developed by applying a smooth spline to the tephra ages and depths in the classical age modelling (CLAM) program (Blaauw 2010; Blair et al. 2015). Our resulting age model has an uncertainty of 5–15 yrs from − 50 to 1200 years BP and an uncertainty of 18–83 years from 1201 to 2000 yrs BP (Fig. 2). The resulting age model was used to estimate changes in sediment accumulation rates over the past 2,000 years.

Lipid analyses

We freeze-dried and extracted sediments using a DionexTM accelerated solvent extraction (ASE 350) system at 120 °C and 1200 psi. We extracted about 3 g of dried sediment for each sample, yielding 1–5 mg of total lipid extracts. We separated all of the extracts with silica gel (40–63 µm, 60 Å) flash chromatography to obtain alkane (hexane; Hex), ketone (dichloromethane; DCM, which contains alkenones), and polar (methanol; MeOH) fractions. Wax esters were removed from the ketone fraction via saponification, in which the fraction was dissolved in a 1 molar potassium hydroxide solution in MeOH:H_2O (95:5, v/v) and heated for 3 h at 65 °C. A solution of 5% NaCl in H_2O was added, followed by acidification using 50% HCl in H_2O. Hex (100%) was then used to extract the desired lipid fraction. Ketone fractions were further purified using silver nitrate columns with a procedure modified from D'Andrea et al. (2007) using DCM (100%) and ethyl acetate (100%). If further cleaning of the alkenone fraction was necessary (as determined through gas-chromatography analyses), a modified urea adduction procedure from Salacup et al. (2019) was used. The ketone fraction was dried under N_2 gas, and dissolved in 1.5 mL of DCM:Hex (2:1, v/v). A 1.5 mL solution of 100 mg/mL urea in MeOH was added, the samples were dried under N_2 gas, and the resulting urea crystals were rinsed with Hex (100%) to remove the non-adduct. The urea crystals were dissolved with Nanopure water, and the resulting adduct was extracted three times using Hex (100%). This process was repeated two additional times, and the cleaned adducts were analyzed. There were several samples with co-eluting compounds that we were unable to remove with this procedure, and in other samples, the alkenone concentrations were too low to measure reliably. These samples were excluded from the final alkenone record.

All alkenones and *n*-alkanes were analyzed with an Agilent 6890 N gas chromatography (GC) system and a flame ionization detector (FID). Alkenones were run on an Agilent VF-200 ms capillary column (60 m × 250 μm × 0.10 μm) and were injected into a CIS-PTV inlet operated in solvent vent mode (6.9 psi at 112 °C). The oven program started at 50 °C, and was then ramped up to 235 °C at 20 °C/min, and ramped again at 1.39 °C/min to 320 °C where it was held isothermally for 5 min. All *n*-alkane samples were run using a Rtx-200 column (105 m × 205 μm × 0.25 μm) and were injected using a pulsed splitless mode (20.3 psi, 310 °C). The oven program was started at 50 °C and was ramped up to 315 °C at 10 °C/min where it was held isothermally for 30 min.

If additional compound identification or verification was required, samples were checked using an Agilent 6890 N GC system coupled with an Agilent 5793 N quadrupole mass spectrometer (MS). Samples were injected using pulsed splitless injection mode (20 psi, 315 °C) and were run on an Agilent VF-200 ms capillary column (60 m × 250 μm × 0.10 μm). The initial oven program was set to 40 °C for 1 min, and was increased to 255 °C at 20 °C/min and again to 315 °C at 2 °C/min where it was held isothermally for 10 min. The MS was set to an ionization energy of 70 eV and a scan range of 50–600 m/z.

Leaf-wax analysis

We used *n*-alkanes to assess changes in algal productivity and regional shifts in vegetation. Typically, shorter chain *n*-alkanes (C_{17}–C_{21}) are associated with phytoplankton (Cranwell et al. 1987). Thus, we can measure changes in C_{17} *n*-alkane fluxes to test for changes in algal productivity. To track vegetation changes in the catchment area, we measured long-chain *n*-alkanes (C_{25}–C_{33}), which are produced by higher-level terrestrial plants (Cranwell 1973; Maffei 1996). Birch trees (e.g. *Betula pubescens* Ehrh. and *Betula nana* L.) produce a high abundance of *n*-alkanes with C_{23}, C_{25}, and C_{27} chain lengths (Schwark et al. 2002; Balascio et al. 2018), whereas herbs and graminoids produce C_{27}, C_{29}, and C_{31} in higher proportions (Cranwell 1973; Maffei 1996; Balascio et al. 2018). To reconstruct shifts in terrestrial vegetation we calculated the average chain length (ACL) for *n*-alkane homologs C_{25}–C_{31} as follows:

$$ACL_{25-31} = \sum \frac{C_i \times [C_i]}{[C_i]} \quad (1)$$

Where C_i represents the *n*-alkane chain length and $[C_i]$ represents *n*-alkane concentrations. Lower ACL values (i.e. an increase in C_{25}-C_{27}) should indicate an increase in birch trees, whereas higher ACL values (i.e. an increase in C_{29}-C_{31}) indicate an increase in herbs and/or grasses.

Alkenones as a proxy for temperature and changes in species distributions

Alkenones are long-chain ketones with varying degrees of unsaturation that are produced by haptophyte algae (i.e. Isochrysidales) in both marine and lacustrine environments. Alkenone-producers can be divided into three main groups, with Group III occurring in marine environments, Group II in both marine and lacustrine environments, and Group I in freshwater lakes (Volkman et al. 1980, 1995; Conte et al. 1995; D'Andrea et al. 2006; Theroux et al. 2010). In all three groups, the distribution of alkenones is correlated with changes in temperature, such that alkenones with a higher degree of unsaturation (e.g.

$C_{37:4}$ Me) are produced in colder environments (Brassell et al. 1986). The U^{K}_{37} and $U^{K'}_{37}$ indices quantify the degree of unsaturation and are correlated to and widely used as proxies for temperature in marine environments (Brassell et al. 1986; Prahl and Wakeham 1987; Prahl et al. 1988; Conte et al. 2006). The U^{K}_{37} index is also applied to lake sediments to reconstruct temperature using different calibrations (Zink et al. 2001; D'Andrea et al. 2011, 2012; Theroux et al. 2013; Randlett et al. 2014; Longo et al. 2016, 2018). The U^{K}_{37} index is calculated as follows:

$$U^{K}_{37} = \frac{[C_{37:2}Me] - [C_{37:4}Me]}{[C_{37:2}Me] + [C_{37:3}Me] + [C_{37:3*}Me] + [C_{37:4}Me]} \qquad (2)$$

Although the U^{K}_{37} index has been used to reconstruct lake temperatures (Zink et al. 2001; D'Andrea et al. 2011, 2012; Randlett et al. 2014), different alkenone producers, in particular Group I versus Group II, can have different U^{K}_{37}-temperature relationships (i.e. species-mixing effects) (Sun et al. 2007; Toney et al. 2012; Theroux et al. 2013; D'Andrea et al. 2016). We can test for impacts of species-mixing on reconstructions using the distinct alkenone signatures produced by Group I Isochrysidales. Group I produces tri-unsaturated isomeric compounds (e.g. $C_{37:3*}$ Me) that can be used to test whether samples contain alkenones produced predominantly by Group I or Group II Isochrysidales. This is calculated using the RIK_{37} index (Longo et al. 2016):

$$RIK_{37} = \frac{[C_{37:3}Me]}{[C_{37:3}Me] + [C_{37:3*}Me]} \qquad (3)$$

A RIK_{37} value of 1.0 indicates that $C_{37:3*}$ Me is not present in the samples and that Group II Isochyrsidales is the main alkenone producer, whereas RIK_{37} values from 0.48 to 0.63 correspond to Group I Isochrysidales (Longo et al. 2016, 2018). Previous surface sediment analyses using alkenones and DNA confirm that Group I Isochyrsidales is the main alkenone producer in VGHV (RIK_{37} = 0.60) in the present day (Longo et al. 2018; Richter et al. 2019).

Group I Isochrysidales has so far only been identified in the Northern Hemisphere and blooms in the spring season during lake ice-off, such that Group I alkenones reflect changes in late winter and spring lake water temperatures (D'Andrea et al. 2011; Longo et al. 2016, 2018). Existing U^{K}_{37}-temperature calibrations provide unreasonable temperature estimates for our alkenone reconstruction. Thus, we present the U^{K}_{37} index as a qualitative estimate of late winter-spring lake water temperatures.

Sedimentological and bulk geochemical data

Physical and geochemical data from VGHV (Blair et al. 2015) was reanalyzed for comparison to our new organic geochemical data. Previous data include wet bulk density, magnetic susceptibility (MS), total organic carbon (TOC), biogenic opal, and total nitrogen (TN) measurements. To account for changes in the sedimentation rate, we calculated flux rates (mg cm^{-2} yr^{-1}) for TOC, TN, and biogenic opal using downcore changes in sediment density measured with a GEOTEK multisensor core logger (MSCL) and sediment accumulation rates from our CLAM age model. Changes in water content and porosity were corrected for by measuring the mass loss before and after samples were freeze-dried. We note that biogenic opal in VGHV was measured using a single extraction method (Mortlock and Froelich 1989) that can be problematic in distinguishing biogenic silica from volcanic glass. Although we assume that the measured silica should predominantly reflect changes in diatom productivity, caution should be used when interpreting these results.

Detection of change-points and transitions

For data analysis, all tephra layers were removed from the sediment depth, and the datasets were re-sampled to the same time intervals with an average resolution of 20 years per sample. We tested whether changes in vegetation composition, sediment inputs, and primary productivity coincided with the historical arrival of Norse settlers in Iceland to determine if human activities were responsible for transitions in terrestrial and aquatic ecosystems in southwest Iceland. To do so, we used the "segmented" package in R version 3.3.3 (R Development Team) to conduct statistical break point analysis on our data to determine the timing of significant changes. A pooled standard error was calculated for each break point to account for age model uncertainties and are reported as 95% confidence intervals. Pearson correlations were also conducted in R.

Results

Short- and long-chain *n*-alkanes as proxies for primary productivity and vegetation

$ACL_{25\text{-}31}$ rapidly increases between 853 ± 10 and 966 ± 9 CE (Fig. 3a, Table 1) reflecting an increase in grasses, sedges, and weeds and a decrease in woody plants, in particular birch trees (*Betula pubescens* ACL_{21-33} = 25.4, and *Betula nana* ACL_{21-33} = 25.6) (Cranwell 1973; Balascio et al. 2018; Maffei et al. 1996). After this shift, $ACL_{25\text{-}31}$ remains stable from 966 ± 9 CE to the present. The C_{17} *n*-alkane flux is slightly higher, but also more variable after c. 1120 ± 74 CE (Fig. 4a). The largest increase in C_{17} occurs after c. 1916 CE, indicating enhanced primary productivity during the twentieth century.

Alkenones as indicators of species-mixing and temperature

The RIK_{37} index suggests that Group I and II are both present in parts of our record. RIK_{37} slightly increases after 514 ± 24 CE, with higher variability after

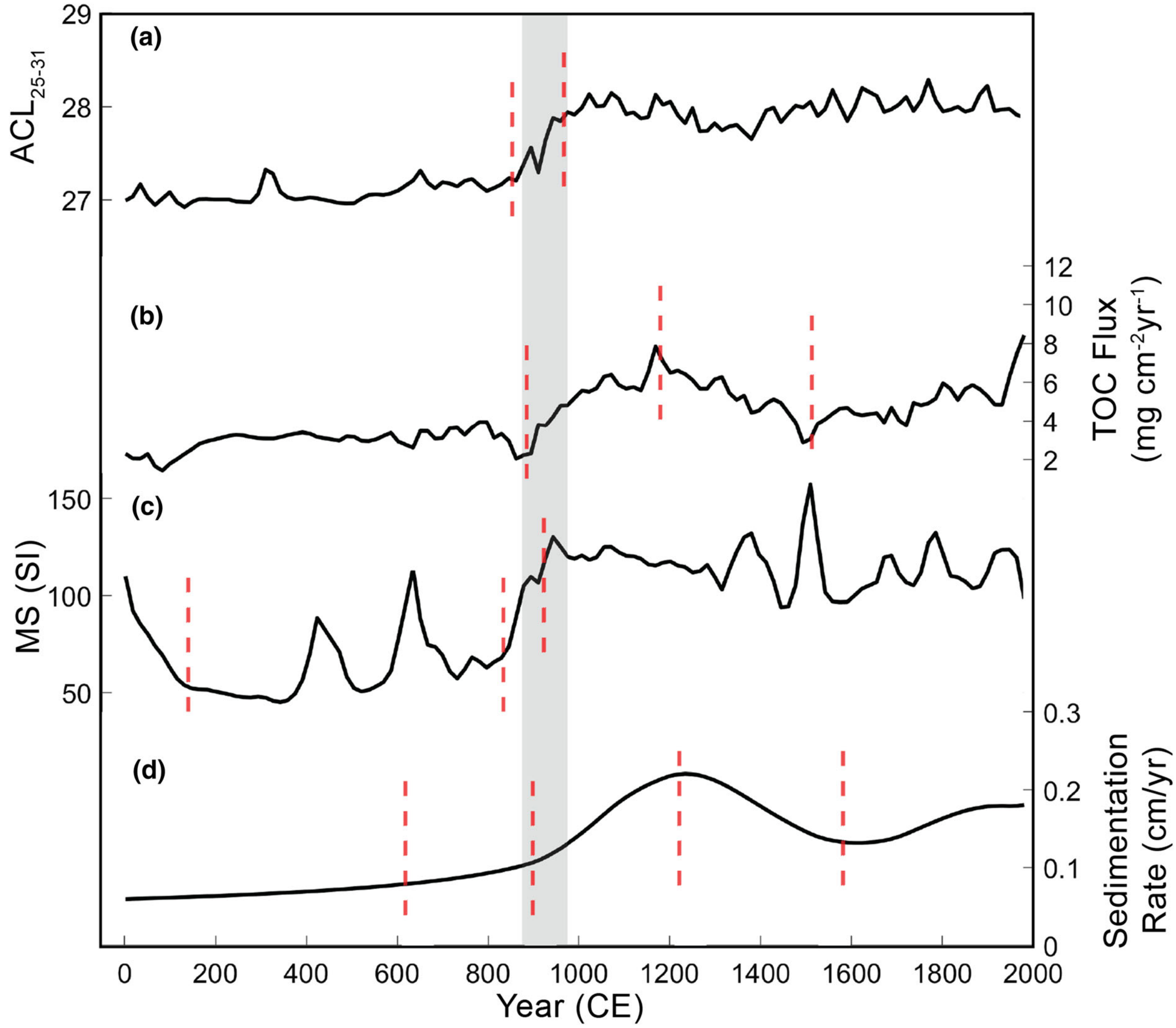

Fig. 3 Reconstructions of changes in the catchment area of VGHV and shifts in sediment composition including (**a**) $ACL_{25\text{-}31}$ indicating shifts in terrestrial vegetation, (**b**) total organic carbon flux (TOC), (**c**) magnetic susceptibility (MS), and (**d**) sedimentation rate. The dashed red lines indicate the break points calculated for each proxy record and the transparent gray bar marks the historic date of *landnám* in Iceland (874 ± 2 CE)

Table 1 Breakpoint analysis for the various proxy records assessed in this study

Variable	Segmented breakpoint analysis	
	Year (CE)	95% CI (±)
$ACL_{25\text{-}31}$	853	10
	966	9
C_{17} flux (mg cm^{-1} yr^{-2})	1120	74
	1916	9
RIK_{37}	514	24
	560	22
	951	22
	1007	20
Magnetic susceptibility (SI)	140	37
	833	15
	922	13
TOC flux (mg cm^{-1} yr^{-2})	884	14
	1180	9
	1513	11
TN flux (mg cm^{-1} yr^{-2})	894	19
	1216	13
	1641	12
Sedimentation rate (cm/yr)	618	22
	898	5
	1222	8
	1581	5
Biogenic opal flux (mg cm^{-1} yr^{-2})	1103	12
	1281	10
	1676	14

951 ± 22 CE (Fig. 4b, Table 1), indicating shifts in the Isochrysidales community from predominantly Group I to both Group I and II over the past c. 1,000 years. Samples with high RIK_{37} values, that is a high abundance of Group II, were removed from the temperature record. After removing these samples, the corrected U^K_{37} and RIK_{37} indices are not correlated ($r = 0.11$, $p = 0.35$). The remaining samples were used to calculate the U^K_{37} index to detect qualitative changes in late winter-spring temperature over time. The U^K_{37} record suggests that late winter-spring temperatures in southwest Iceland were gradually increasing over the past 2,000 years.

Re-analysis of physical and bulk organic and inorganic data

Although tephras were removed from our sediment stratigraphy, there are remnants of large volcanic eruptions in the MS signal (Fig. 3d). This includes eruptions that occurred at c. 39 BCE, 58 CE, 435 CE, 452 CE, 617 CE, and 1500 CE. The largest shift in MS occurs after c. 833 ± 15 CE and is coincident with increases in TOC flux (884 ± 14 CE), TN flux (894 ± 19 CE), and sedimentation rate (898 ± 5 CE) (Table 1, Figs. 3 and 4). An increase in biogenic opal commences about 1103 ± 12 CE and peaks c. 1281 ± 10 CE. This generally coincides with peaks in TOC (c. 1180 ± 9 CE) and TN fluxes (c. 1216 ± 13 CE). The decrease in biogenic opal, TOC, and TN fluxes coincide with decreasing sedimentation rates after c. 1222 ± 8 CE. Similarly, increasing sedimentation rates c. 1581 ± 5 CE correspond to increases in biogenic opal (c. 1676 ± 14 CE), TOC (c. 1513 ± 11 CE), and TN (c. 1641 ± 12 CE).

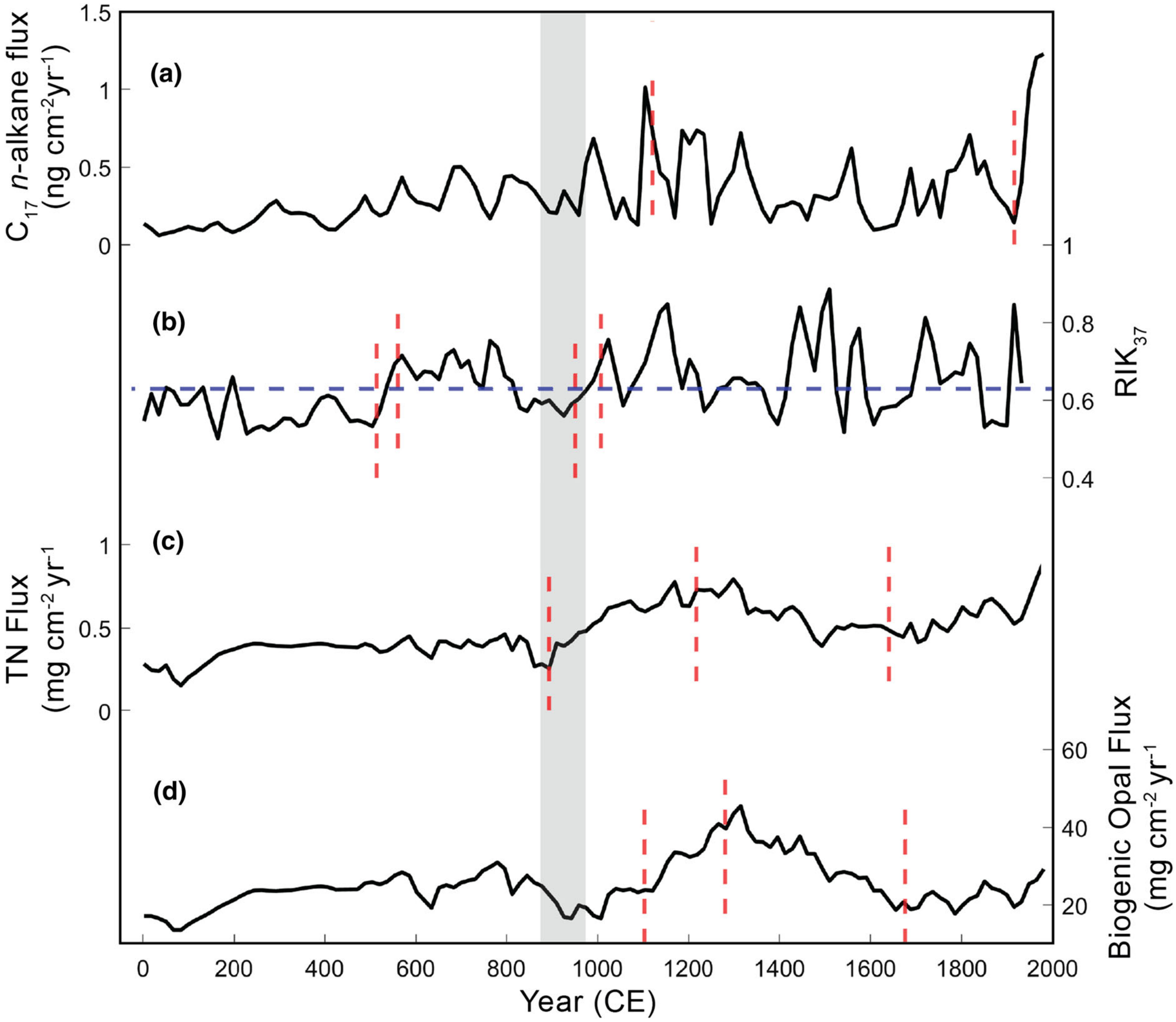

Fig. 4 Shifts in VGHV (**a**) primary productivity as indicated by the C_{17} *n*-alkane flux and changes within the (**b**) Isochrysidales community between Group I (RIK_{37} = 0.48–0.63) and Group II (RIK_{37} = 1.0). The blue dashed line corresponds to the empirically defined cut-off for Group I (RIK_{37} = 0.63). Group I is solely present in samples with RIK_{37} values below 0.63 and Group II is present in samples where RIK_{37} values exceed 0.63. These changes are compared with shifts in (**c**) total nitrogen (TN) deposition and (**d**) biogenic opal flux as a proxy for diatom productivity. The dashed red lines mark the break points for the different proxy records and the gray bar corresponds to *landnám* in Iceland (874 ± 2 CE). (Color figure online)

Discussion

Climatic and ecological changes prior to Norse settlement

Decreasing summer solar insolation led to long-term cooling in Northern Europe over the past c. 6,000–5,000 years BP. This is typically associated with a decrease in Fennoscandian forest extent (Seppä et al. 2009). Similarly, in Greenland and the Faroe Islands woody vegetation decreased after c. 3,000 years BP (Hannon et al. 2005; Massa et al. 2012b). Our U^K_{37} temperature record from VGHV, however, suggests late winter and spring warming during this time, likely due to rising winter-spring insolation. There is also evidence for centennial climate variability in the VGHV U^K_{37} record and marine temperature reconstructions, with warming during the Roman Warm Period (RWP, c. 250 BCE-400 CE) and cooling during the Dark Ages Cold Period (DACP, c. 450–550 CE)

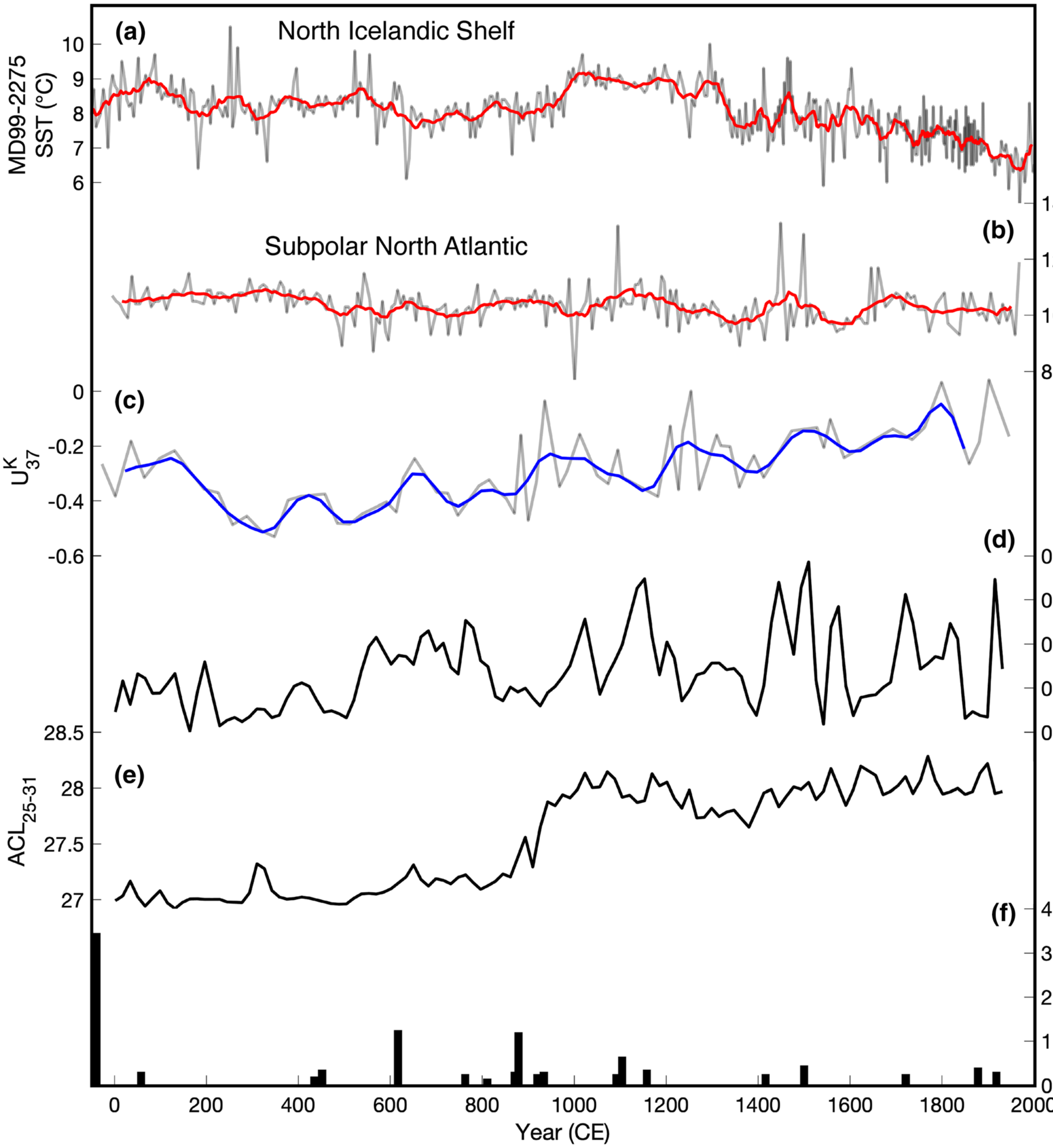

Fig. 5 Alkenone temperature reconstructions in marine sediment records from (**a**) the North Icelandic shelf (Sicre et al. 2008, 2011) and (**b**) the subpolar North Atlantic (Sicre et al. 2011). For comparison, the (**c**) U^K_{37} winter-spring temperature reconstruction from VGHV is shown. Environmental changes in the lake are reflected by (**d**) RIK_{37} values and shifts in terrestrial vegetation are indicated by (**e**) $ACL_{25\text{-}31}$. Volcanic tephra deposition in VGHV is displayed as (**f**) tephra thickness

(Fig. 5) (Sicre et al. 2008, 2011; Seppä e al. 2009). Yet the relative abundance of birch trees and herb/grasses in southwest Iceland remain stable between c. 0 and 870 CE. In addition, there are no significant changes in VGHV primary productivity (i.e. biogenic opal and C_{17} *n*-alkanes) prior to *landnám* (Fig. 4).

There is, however, a slight increase in the RIK_{37} values c. 514–560 CE, which could indicate that Group II Isochrysidales was present in the lake in low abundance (Fig. 5d) (Longo et al. 2018). Previous studies suggest that shifts in Group I and II Isochrysidales communities are primarily driven by changes in salinity, with Group I only present at 0–0.5 practical salinity units (psu) and Group I and Group II present at 0.5–5 psu (Longo et al. 2016). VGHV is a freshwater lake (0.1 psu) and given the low chemical weathering rates in the cool Icelandic climate, salt fluxes to the lake are very low. It is unlikely that short-term climate fluctuations would promote high enough evaporation rates to result in large salinity changes. Alternatively, the RIK_{37} values during this time period could correspond to Group I Isochrysidales but are outside of the recorded empirical range.

Prior to *landnám*, several major volcanic eruptions occurred in Iceland at 39 BCE, and subsequent eruptions in 58 CE, 435 CE, 452 CE, and 617 CE resulted in distinct tephra layers in VGHV (Fig. 5f) and increases in MS (Blair et al. 2015). VGHV sedimentation rate increased after c. 600 CE, which could be associated with a volcanic eruption that occurred c. 617 CE and triggered long-term reworking of the volcanic tephra layer or localized soil erosion from breaks in vegetation (Dugmore et al. 2005, 2009). Alternatively, gradual increases in erosion could be caused by long-term Neoglacial cooling trends that are associated with increased glacial activity and heightened wind erosion (Jennings et al. 2001; Dugmore et al. 2005, 2009; Geirsdóttir et al. 2009, 2013; Blair et al. 2015).

Existing paleo-reconstructions from Iceland disagree as to whether climate change led to a decrease in forest extent (Ólafsdóttir et al. 2001) and increased soil erosion (Geirsdóttir et al. 2009, 2013) prior to *landnám*, or if Norse settlers are responsible for the rapid decline in birch trees and accelerated soil erosion (Dugmore et al. 2009; Streeter et al. 2015). The VGHV record from southwest Iceland suggests that overall the landscape was relatively stable and that there were no major aquatic shifts in response to climate perturbations or volcanic eruptions prior to Norse settlement.

Environmental impacts of the Medieval Climate Anomaly and Norse settlement

Viking expansion and settlement of North Atlantic islands is thought to have occurred during a mild and relatively warm climate, typically referred to as the Medieval Climate Anomaly (MCA; c. 950–1250 CE) (Ogilvie et al. 2000; Sëppa et al. 2009). Our U^K_{37} winter-spring temperature record indicates slight warming interspersed with brief cold anomalies between c. 900–1100 CE, whereas summer reconstructions suggest that peak warming occurred c. 1000–1300 CE (Fig. 5) (Ogilvie et al. 2000; Sicre et al. 2008, 2011; Gathorne-Hardy et al. 2009; Holmes et al. 2016). This gradual warming coincides with an abrupt shift in the VGHV $ACL_{25\text{-}31}$ record, indicating a rapid decline in birch trees between c. 853–966 CE. Similarly, pollen records from Iceland, including data from a low-resolution record from VGHV, suggest that birch woodlands in southern Iceland disappeared rapidly c. 870–920 CE and were replaced by grasses, sedges, and dwarf-shrub heath (Hallsdóttir 1987; Dugmore et al. 2005; Hallsdóttir and Caseldine 2005). This corresponds to the timing of Norse settlement in Iceland and introduction of agricultural practices that included extensive land clearance (Dugmore et al. 2005). A very similar situation was observed in Greenland, with a rapid decline in woody vegetation shortly after settlement (Fig. 6) (Massa et al. 2012a).

The decline of birch trees coincides with increases in MS and sedimentation rates recording heightened erosion and minerogenic inputs shortly after human settlement in 874 ± 2 CE (Fig. 3). Some of the initial changes in sedimentation rate and MS could be associated with the *landnám* tephra (871 ± 2 CE), but both sedimentation rate and MS remain high after the volcanic eruption, indicating that human and/or climatic impacts led to sustained changes in the catchment area. In the Eastern Norse settlement of southern Greenland, soil erosion rates also increased shortly after *landnám*, which is associated with land clearance and the introduction of sheep to the landscape (Edwards et al. 2008; Massa et al. 2012a).

Major changes in VGHV productivity (i.e. C_{17} *n*-alkane and biogenic opal fluxes), as well as changes in the RIK_{37} values, occur between c. 950 and 1150 CE (Fig. 4). Increased primary productivity is potentially due to higher nutrient inputs associated with soil erosion and deforestation, and/or grazing and other agricultural processes (manuring). Although shifts in the haptophyte community are commonly thought to be driven by salinity, our observation of increased Group II abundance at this time fits with increases in Group II alkenone production observed in anthropogenically influenced lakes from northeast China (Yao et al. 2019). In northern Iceland, productivity

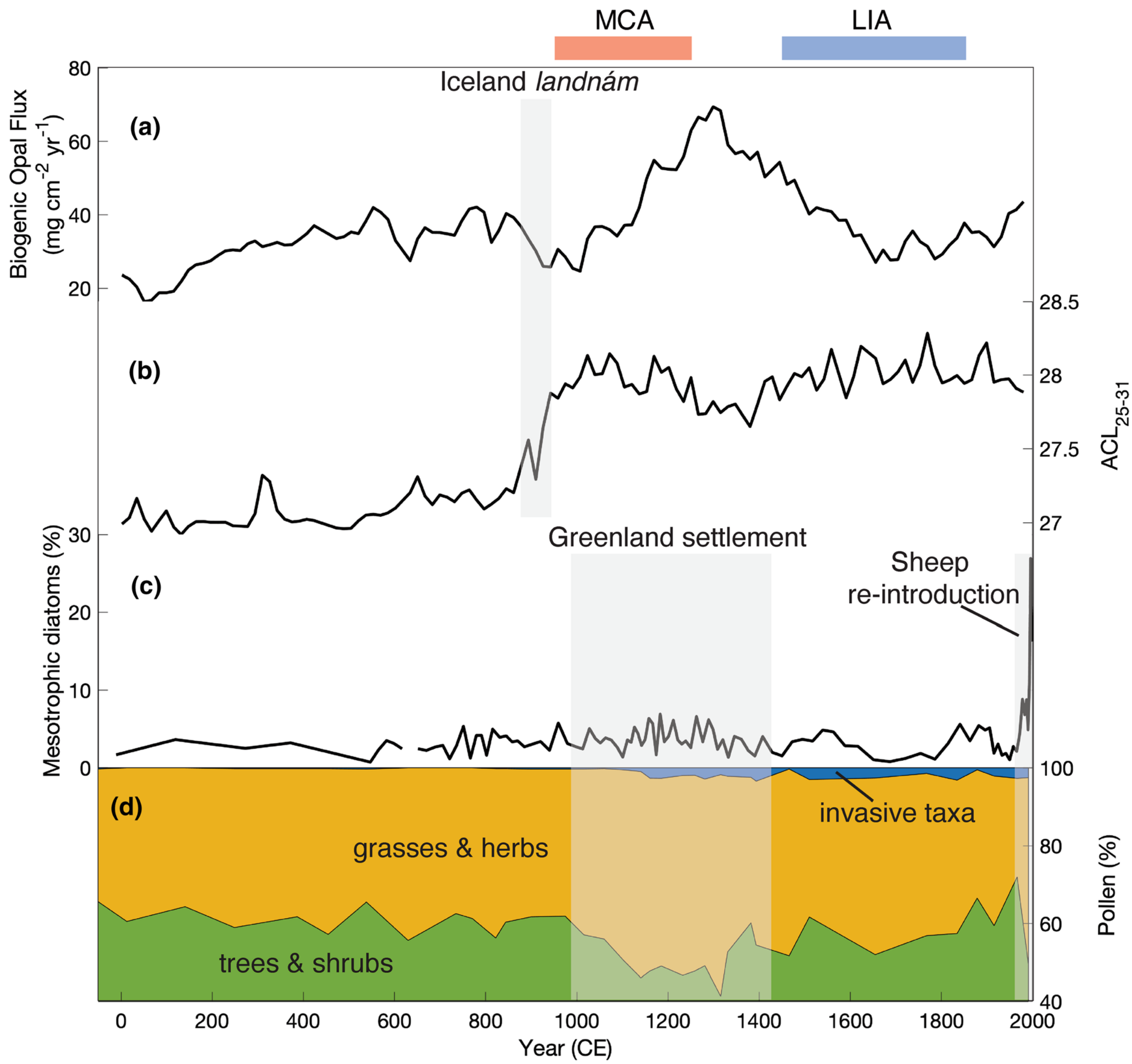

Fig. 6 Changes in VGHV (**a**) biogenic opal (i.e. diatoms) and (**b**) ACL_{25-31} (i.e. terrestrial vegetation), compared with ecological shifts in Greenland after the Norse settlement near lake Igaliku are reflected by (**c**) mesotrophic diatom species and (**d**) plant types (Massa et al. 2012a). The timing of the Medieval Climate Anomaly (MCA) and Little Ice Age (LIA) are indicated

also increases shortly after *landnám* in Lake Helluvaðstjörn; however, there are no corresponding increases in soil erosion (Lawson et al. 2007). Heightened nutrient inputs into Lake Helluvaðstjörn are attributed to either forest clearance, resulting in more nutrient leaching from soils, or the introduction of livestock (Lawson et al. 2007). Previous studies suggest that lakes and rivers in Iceland, particularly in southwest Iceland, are often nitrogen-limited due to inputs of phosphorous from the chemical weathering of basalt (Jónasson et al. 1992; Gíslason et al. 1996). The introduction of livestock and increased nitrogen-fertilization from manure could therefore be particularly important in promoting increased algal productivity in Icelandic lakes. This is also observed in lakes on the Faroe Islands, also composed of basalt, where there was minimal forest cover prior to human settlement, yet productivity in many lakes increased from nutrient loading post-settlement (Hannon et al. 2005; Lawson et al. 2005). This contrasts to a settlement in southern Greenland, a granitic terrain, where there were no noticeable impacts on the trophic state of the lake as evidenced by stability in diatom species and no obvious changes in algal production (Fig. 6) (Massa et al. 2012a). Although these results suggest livestock introduction could have disproportionate impacts on productivity in lakes in basaltic terrains, it is difficult to directly compare these examples, since the intensity and style of land-use change differs in the different environments, and pre-anthropogenic nutrient concentrations are uncertain. Nevertheless, with some exceptions, increased lacustrine primary production appears to be a widespread response to Norse settlement in the North Atlantic, with or without large changes in terrestrial vegetation.

Certain proxies, such as TOC and biogenic opal, are often used to reconstruct climate assuming that a warmer climate heightens lacustrine primary productivity (Geirsdóttir et al. 2009, 2013; Blair et al. 2015). Although there is a weak correlation between C_{17} *n*-alkane fluxes and our U^{K}_{37} temperature record ($r = 0.20$, $p < 0.05$), there is no correlation between biogenic opal and the U^{K}_{37} index. In addition, simultaneous increases in $ACL_{25\text{-}31}$, MS, and sedimentation rate followed by increases in C_{17} *n*-alkane and biogenic opal fluxes in the VGHV environmental record coincide with the historical settlement of the Norse. Our results suggest that human settlement dominated terrestrial and aquatic ecosystem changes in the last ~ 1,100 years in southwest Iceland.

Post-settlement era and the Little Ice Age

The post-settlement period in Iceland and Greenland, along with settlements in Northern Norway, took different trajectories as the settlers, terrestrial, and aquatic ecosystems adjusted to changes in local climate and human activities. In the VGHV $ACL_{25\text{-}31}$ record, vegetation dominated by grasses, sedges, and dwarf-shrub heath stabilized after c. 966 CE, in contrast to the abundant birch trees observed prior to human settlement. In contrast, vegetation in northern Norway fluctuated between forests and agricultural types depending on changes in climate and human land-use (Balascio and Wickler 2018). In Greenland, either environmental degradation, socioeconomic issues, or climatic changes resulted in the rapid demise of Norse settlements in the fourteenth century (Edwards et al. 2008; Massa et al. 2012a). The abandonment of these settlements allowed for the recovery of native vegetation (i.e. the birch woodlands) and a decrease in soil erosion rates (Fig. 5) (Massa et al. 2012a). In contrast, the Icelandic settlers withstood both environmental degradation of the landscape and fluctuations in climate.

Despite the continued presence of Norse settlers in Iceland, sedimentation rates decreased c. 1222 CE before increasing again c. 1581 CE. The temporary decline in erosion could be associated with stabilization of soils after initial changes in vegetation or less intensive land-use practices (Hallsdóttir and Caseldine 2005; Dugmore et al. 2006). The VGHV MS record, however, remains relatively stable during the post-settlement era (aside from brief increases in MS shortly after tephras). These divergent lines of evidence could be reconciled if MS responds not only to total clastic sediment inputs but also to the composition of those inputs, such as magnetite (Bradshaw and Thompson 1985; Hawley et al. 2017). The depletion of soils via erosion during Norse colonization could have mobilized large quantities of surface material to the lake that were relatively enriched in magnetite (Óskarsson et al. 2012; Hawley et al. 2017). Increases in sedimentation rates in the latter half of the last millennium are observed in numerous terrestrial and marine records in Iceland and are attributed to a cooling climate and heightened erosion rates from increased periglacial activity and windiness during the Little Ice Age (LIA) (Jennings et al. 2001; Sicre et al. 2008; Geirsdóttir et al. 2009, 2013; Streeter et al. 2015).

Heightened VGHV diatom productivity only lasts for a few centuries before gradually decreasing between c. 1300–1700 CE, whereas RIK_{37} and C_{17} values become more variable (Fig. 4). Similarly, in northeast Iceland chironomid concentrations start to decrease c. 1200 CE, and algal productivity also declines (Lawson et al. 2007). This roughly corresponds to the end of the MCA as observed in several marine and terrestrial records (although this is not reflected in the winter-spring VGHV temperature reconstruction) (Fig. 5) (Sicre et al. 2008, 2011; Gathorne-Hardy et al. 2009; Holmes et al. 2016). Rather, winter-spring temperatures suggest there was a slight cooling c. 1200 CE, followed by increased climate variability. This change in primary productivity could indicate seasonal shifts in temperature that directly influenced changes in lacustrine ecosystems, or a reduction in human activities in the landscape (Ogilvie et al. 2000). Peaks in algal productivity in a northeastern Icelandic lake after c. 1700 CE and the rapid increase in C_{17} *n*-alkane flux in VGHV after c. 1900 CE, could be related to either heightened nutrient inputs from increased agricultural activity in the catchment area and/or climate changes (Lawson et al. 2007). Thus, climate could have played a role in driving some of the centennial-scale environmental changes observed during the LIA, including changes in primary productivity within the lake and soil erosion.

Conclusions

Concurrent analyses of proxies that reflect climate and environmental changes provide new insights into how and why the Icelandic landscape changed over the past 2,000 years. Prior to Norse settlement (c. 0–870 CE), the lack of major changes in the VGHV catchment area or in primary productivity indicate that climate and volcanic eruptions did not have a significant influence on the terrestrial and aquatic ecosystems. There is some evidence of increased soil erosion, which could be an artifact of either gradual cooling or volcanic eruptions. However, the most severe and rapid environmental shifts in southwest Iceland took place shortly after Norse settlement. The $ACL_{25\text{-}31}$ record provides an integrated perspective on the rate and magnitude of bulk vegetation changes in Iceland. In particular, there is a permanent shift in vegetation composition that is accompanied by a rapid increase in soil erosion. Changes in the aquatic ecosystem were less stable and fluctuated more frequently after human settlement. This indicates that human activities were the primary drivers of environmental change in southwest Iceland after c. 870 CE, and these effects were exacerbated by climate and volcanic eruptions. Thus, caution should be used when interpreting and calibrating proxies that are sensitive to human induced changes, climate variability, and/or volcanic eruptions. Finally, the continued increase in primary productivity over the past century, suggests that human activities and/or a warming climate might lead to future environmental issues (e.g. eutrophication) in Icelandic lakes.

Acknowledgements This work was supported by the Geological Society of America Graduate Student Research Grants, the Nicole Rosenthal Hartnett Graduate Fellowship, along with funding from the Brown University Graduate School. Lake sediments for this project were obtained from LacCore (National Lacustrine Core Facility), Department of Earth Sciences, University of Minnesota-Twin Cities. In addition, we would like to thank R. Rose and Prof. T. Herbert for analytical support and advice, Dr. J. Salacup, and Dr. G. Weiss for advice. We would also like to thank the Brown University Undergraduate Training and Research Awards for supporting this work. All new data presented in this paper will be available through the National Oceanic and Atmospheric Administration World Data Service for Paleoclimatology.

References

Balascio NL, D'Andrea WJ, Anderson RS, Wickler S (2018) Influence of vegetation type on *n*-alkane composition and hydrogen isotope values from a high latitude ombrotrophic bog. Org Geochem 121:48–57

Balascio NL, Wickler S (2018) Human–environment dynamics during the Iron Age in the Lofoten Islands, Norway. Nor J Geogr 72:146–160

Blaauw M (2010) Methods and code for 'classical' age-modelling of radiocarbon sequences. Quat Geochronol 5:512–518

Blair CL, Geirsdóttir Á, Miller GH (2015) A high-resolution multi-proxy lake record of Holocene environmental change in southern Iceland. J Quat Sci 30:281–292

Bradshaw R, Thompson R (1985) The use of magnetic measurements to investigate the mineralogy of Icelandic lake sediments and to study catchment processes. Boreas 14:203–215

Brassell SC, Eglinton G, Marlowe IT, Pflaumann U, Sarnthein M (1986) Molecular stratigraphy: a new tool for climatic assessment. Nature 320:129–133

Christensen CL (2013) Multi-proxy responses of Icelandic lakes to Holocene tephra perturbations. Master's thesis, University of Colorado, Boulder

Cranwell P, Eglinton G, Robinson N (1987) Lipids of aquatic organisms as potential contributors to lacustrine sediments: ii. Org Geochem 11:513–527

Cranwell PA (1973) Chain-length distribution of *n*-alkanes from lake sediments in relation to post-glacial environmental change. Freshw Biol 3:259–265

Conte MH, Sicre MA, Rühlemann C, Weber JC, Schulte S, Schulz-Bull D, Blanz T (2006) Global temperature calibration of the alkenone unsaturation index (U37K') in surface waters and comparison with surface sediments. Geochem Geophys Geosy. https://doi.org/10.1029/2005GC001054

Conte MH, Thompson A, Eglinton G, Green JC (1995) Lipid biomarker diversity in the coccolithophorid *Emiliania huxleyi* (Prymnesiophyceae) and the related species *Gephyrocapsa oceanica*. J Phycol 31:272–282

D'Andrea WJ, Huang Y, Fritz SC, Anderson NJ (2011) Abrupt Holocene climate change as an important factor for human

migration in West Greenland. Proc Natl Acad Sci 108:9765–9769
D'Andrea WJ, Lage M, Martiny JB, Laatsch AD, Amaral-Zettler LA, Sogin ML, Huang Y (2006) Alkenone producers inferred from well-preserved 18S rDNA in Greenland lake sediments. J Geophy Res Biogeo. https://doi.org/10.1029/2005JG000121
D'Andrea WJ, Liu Z, Alexandre MDR, Wattley S, Herbert TD, Huang Y (2007) An efficient method for isolating individual long-chain alkenones for compound-specific hydrogen isotope analysis. Anal Chem 79:3430–3435
D'Andrea WJ, Theroux S, Bradley RS, Huang X (2016) Does phylogeny control U^{K}_{37}-temperature sensitivity? Implications for lacustrine alkenone paleothermometry. Geochim Cosmochim Acta 175:168–180
D'Andrea WJ, Vaillencourt DA, Balascio NL, Werner A, Roof SR, Retelle M, Bradley RS (2012) Mild Little Ice Age and unprecedented recent warmth in an 1800 year lake sediment record from Svalbard. Geology 40:1007–1010
Dugmore AJ, Church MJ, Buckland PC, Edwards KJ, Lawson I, McGovern TH, Panagiotakopulu E, Simpson IA, Skidmore P, Sveinbjarnardóttir G (2005) The Norse *landnám* on the North Atlantic islands: an environmental impact assessment. Polar Rec 4:21–37
Dugmore AJ, Church MJ, Mairs KA, McGovern TH, Newton AJ, Sveinbjarnardóttir G (2006) An over-optimistic pioneer fringe? environmental perspectives on medieval settlement abandonment in Þórsmörk. Aarhus University Press, South Iceland
Dugmore AJ, Gísladóttir G, Simpson IA, Newton A (2009) Conceptual models of 1200 years of Icelandic soil erosion reconstructed using tephrochronology. J North Atl 2:1–19
Edwards KJ, Schofield JE, Mauquoy D (2008) High resolution paleoenvironmental and chronological investigations of Norse *landnám* at Tasiusaq, Eastern Settlement, Greenland. Quat Res 69:1–15
Gathorne-Hardy FJ, Erlendsson E, Langdon PG, Edwards KJ (2009) Lake sediment evidence for late Holocene climate change and landscape erosion in western Iceland. J Paleolimnol 42:413–426
Geirsdóttir Á, Miller GH, Larsen DJ, Ólafsdóttir S (2013) Abrupt Holocene climate transitions in the northern North Atlantic region recorded by synchronized lacustrine records in Iceland. Quat Sci Rev 70:48–62
Geirsdóttir Á, Miller GH, Thordarson T, Ólafsdóttir KB (2009) A 2000 year record of climate variations reconstructed from Haukadalsvatn, West Iceland. J Paleolimnol 41:95–115
Gíslason SR, Arnórsson S, Ármannsson H (1996) Chemical weathering of basalt in Southwest Iceland: effects of runoff, age of rocks and vegetative/glacial cover. Am J Sci 296:837–907
Hallsdóttir M (1987) Pollen analytical studies of human influence on vegetation in relation to the landnám tephra layer in southwest Iceland. Doctoral dissertation, Lund University, Lund
Hallsdóttir M, Caseldine CJ (2005) The Holocene vegetation history of Iceland, state-of-the-art and future research. Dev Quat Sci 5:319–334
Hannon GE, Bradshaw RH, Bradshaw EG, Snowball I, Wastegård S (2005) Climate change and human settlement as drivers of late-Holocene vegetational change in the Faroe Islands. Holocene 15:639–647
Hawley SM, von Strandmann PAP, Burton KW, Williams HM, Gíslason SR (2017) Continental weathering and terrestrial (oxyhydr)oxide export: Comparing glacial and non-glacial catchments in Iceland. Chem Geol 462:55–66
Hjartarson A, Sæmundsson K (2014) Geological map of Iceland–bedrock map,1:600 000, datum: Isn 93. Iceland GeoSurvey, Reykjavik
Holmes N, Langdon PG, Caseldine CJ, Wastegård S, Leng MJ, Croudace IW, Davies SM (2016) Climatic variability during the last millennium in Western Iceland from lake sediment records. Holocene 26:756–771
Jennings AE, Hagen S, Harðardóttir J, Stein R, Ogilvie AE, Jónsdóttir I (2001) Oceanographic change and terrestrial human impacts in a post AD 1400 sediment record from the southwest Iceland shelf. Clim Chang 48:83–100
Jónasson PM, Adalsteinsson H, St. Jónsson G, (1992) Production and nutrient supply of phytoplankton in subarctic, dimictic Thingvallavatn, Iceland. Oikos 64:162–187
Lawson IT, Church MJ, McGovern TH, Arge SV, Woollet J, Edwards KJ, Gathorne-Hardy FJ, Dugmore AJ, Cook G, Mairs KA, Thomson AM (2005) Historical ecology on Sandoy, Faroe Islands: palaeoenvironmental and archaeological perspectives. Hum Ecol 33:651–684
Lawson IT, Gathorne-Hardy FJ, Church MJ, Newton AJ, Edwards KJ, Dugmore AJ, Einarsson A (2007) Environmental impacts of the Norse settlement: palaeoenvironmental data from Mývatnssveit, Northern Iceland. Boreas 36:1–19
Longo WM, Huang Y, Yao Y, Zhao J, Giblin AE, Wang X, Zech R, Haberzettl T, Jardillier L, Toney J, Liu Z, Krivonogov S, Kolpakova M, Chu G, D'Andrea WJ, Harada N, Nagashima K, Sato M, Yonenobu H, Yamada K, Gotanda K, Shinozuka Y (2018) Widespread occurrence of distinct alkenones from Group I haptophytes in freshwater lakes: Implications for paleotemperature and paleoenvironmental reconstructions. Earth Planet Sci Lett 492:239–250
Longo WM, Theroux S, Giblin AE, Zheng Y, Dillon JT, Huang Y (2016) Temperature calibration and phylogenetically distinct distributions for freshwater alkenones: evidence from northern Alaskan lakes. Geochim Cosmochim Acta 180:177–196
Maffei M (1996) Chemotaxonomic significance of leaf wax alkanes in the Gramineae. Biochem Syst Ecol 24:53–64
Massa C, Bichet V, Gauthier É, Perren BB, Mathieu O, Petit C, Monna F, Giraudeau J, Losno R, Richard H (2012a) A 2500 year record of natural and anthropogenic soil erosion in South Greenland. Quat Sci Rev 32:119–130
Massa C, Perren BB, Gauthier E, Bichet V, Petit C, Richard H (2012b) A multiproxy evaluation of Holocene environmental change from Lake Igaliku, South Greenland. J Paleolimnol 48:241–258
McKendrigk JD, Batzli GO, Everett KR, Swanson JC (1980) Some effects of mammalian herbivores and fertilization on tundra soils and vegetation. Arct Alp 12:565–578
Mortlock RA, Froelich PN (1989) A simple method for the rapid determination of biogenic opal in pelagic marine sediments. Deep-Sea Res Part I Oceanogr Res Pap 36:1415–1426

Ogilvie AE, Barlow LK, Jennings AE (2000) North Atlantic climate c. AD 1000: Millennial reflections on the Viking discoveries of Iceland. Greenl N Am Weather 55:34–45

Ólafsdóttir R, Schlyter P, Haraldsson HV (2001) Simulating Icelandic vegetation cover during the Holocene implications for long-term land degradation. Geogr Ann Phys Geogr 83:203–215

Óskarsson BV, Riishuus MS, Arnalds Ó (2012) Climate-dependent chemical weathering of volcanic soils in Iceland. Geoderma 189:635–651

Prahl FG, Muehlhausen LA, Zahnle DL (1988) Further evaluation of long-chain alkenones as indicators of paleoceanographic conditions. Geochim Cosmochim Acta 52:2303–2310

Prahl FG, Wakeham SG (1987) Calibration of unsaturation patterns in long-chain ketone compositions for palaeotemperature assessment. Nature 330:367–369

Randlett MÈ, Coolen MJ, Stockhecke M, Pickarski N, Litt T, Balkema C, Kwiecien O, Tomonaga Y, Wehrli B, Schubert CJ (2014) Alkenone distribution in Lake Van sediment over the last 270 ka: influence of temperature and haptophyte species composition. Quat Sci Rev 104:53–62

Richards JD (2005) The Vikings: a very short introduction. Oxford University Press, New York

Richter N, Longo WM, George S, Shipunova A, Huang Y, Amaral-Zettler L (2019) Phylogenetic diversity in freshwater-dwelling Isochrysidales haptophytes with implications for alkenone production. Geobiology 17:272–280

Salacup JM, Farmer JR, Herbert TD, Prell WL (2019) Alkenone paleothermometry in coastal settings: Evaluating the potential for highly resolved time series of sea surface temperature. Paleoceanogr Paleocl 34:164–181

Schwark L, Zink K, Lechterbeck J (2002) Reconstruction of postglacial to early Holocene vegetation history in terrestrial Central Europe via cuticular lipid biomarkers and pollen records from lake sediments. Geology 30:463–466

Seppä H, Bjune AE, Telford RJ, Birks HJB, Veski S (2009) Last nine-thousand years of temperature variability in Northern Europe. Clim Past 5:523–535

Sicre MA, Hall IR, Mignot J, Khodri M, Ezat U, Truong MX, Eiríksson J, Knudsen KL (2011) Sea surface temperature variability in the subpolar Atlantic over the last two millennia. Paleoceanography. https://doi.org/10.1029/2011PA002169

Sicre MA, Jacob J, Ezat U, Rousse S, Kissel C, Yiou P, Eiríksson J, Knudsen KL, Jansen E, Turon JL (2008) Decadal variability of sea surface temperatures off North Iceland over the last 2000 years. Earth Planet Sci Lett 268:137–142

Streeter R, Dugmore AJ, Lawson IT, Erlendsson E, Edwards KJ (2015) The onset of the palaeoanthropocene in Iceland: Changes in complex natural systems. Holocene 25:1662–1675

Sun Q, Chu G, Liu G, Li S, Wang X (2007) Calibration of alkenone unsaturation index with growth temperature for a lacustrine species, *Chrysotila lamellosa* (Haptophyceae). Org Geochem 38:1226–1234

Theroux S, D'Andrea WJ, Toney J, Amaral-Zettler L, Huang Y (2010) Phylogenetic diversity and evolutionary relatedness of alkenone-producing haptophyte algae in lakes: implications for continental paleotemperature reconstructions. Earth Planet Sci Lett 300:311–320

Theroux S, Toney J, Amaral-Zettler L, Huang Y (2013) Production and temperature sensitivity of long chain alkenones in the cultured haptophyte *Pseudoisochrysis paradoxa*. Organ Geochem 62:68–73

Toney JL, Theroux S, Andersen RA, Coleman A, Amaral-Zettler L, Huang Y (2012) Culturing of the first 37:4 predominant lacustrine haptophyte: geochemical, biochemical, and genetic implications. Geochim Cosmochim 78:51–64

Volkman JK, Barrerr SM, Blackburn SI, Sikes EL (1995) Alkenones in *Gephyrocapsa oceanica*: Implications for studies of paleoclimate. Geochim Cosmochim Acta 59:513–520

Volkman JK, Eglinton G, Corner ED, Forsberg TEV (1980) Long-chain alkenes and alkenones in the marine coccolithophorid *Emiliania huxleyi*. Phytochemistry 19:2619–2622

Yao Y, Zhao J, Longo WM, Li G, Wang X, Vachula RS, Wang KJ, Huang Y (2019) New insights into environmental controls on the occurrence and abundance of Group I alkenones and their paleoclimate applications: evidence from volcanic lakes of northeastern China. Earth Planet Sci Lett 527:115792

Zink KG, Leythaeuser D, Melkonian M, Schwark L (2001) Temperature dependency of long-chain alkenone distributions in recent to fossil limnic sediments and in lake waters. Geochim Cosmochim Acta 65:253–265

Zori D (2016) The Norse in Iceland. Oxford University Press, London